ELSEVIER

Journal of Organometallic Chemistry 554 (1998) 75–85

Journal of Organometallic Chemistry

# Photochemistry of bis-{chloro(dicarbonyl)rhodium} in low temperature frozen gas matrices at 12 K and in Nujol mulls at 77 K: infrared and electronic spectroscopic evidence for retention of the bis-{(chloro)rhodium} bridging unit but photoejection of terminal carbonyl ligands

J. Timothy Bays [a], Thomas E. Bitterwolf [a,*], Kimberley A. Lott [a], Mario A. Ollino [b,1], Antony J. Rest [b,2], Lisa M. Smith [b]

[a] *Department of Chemistry, University of Idaho, Moscow, ID 83843, USA*
[b] *Department of Chemistry, The University, Southampton, SO17 1BJ, UK*

Received 9 January 1997; received in revised form 3 June 1997

**Abstract**

Infrared and electronic spectroscopic evidence is presented in relation to the photochemical reactions of $\{(Cl)(CO)_2Rh\}_2$, whose bent structure has been confirmed by Fourier transform Raman spectroscopy. Photolysis in Ar, $CH_4$ and $N_2$ gas matrices at ca. 12 K and in Nujol mulls at ca. 77 K leads to facile and reversible ejection of the terminal CO ligands but retention of the $\{(Cl)Rh\}_2$ bridging unit. The primary species formed were $Rh_2(Cl)_2(CO)_3$ in Ar, $CH_4$ and Nujol media and $Rh_2(Cl)_2(CO)_3(N_2)$ in $N_2$ matrices. Further reversible CO loss afforded $\{Rh(Cl)(CO)\}_2$ and $\{Rh(Cl)(CO)(N_2)\}_2$, respectively. In CO matrices the modest photoreaction was interpreted in terms of CO addition to give an 18 electron dimeric species $\{Rh(Cl)(CO)_3\}_2$ rather than bridge cleavage to give the 16 electron species $Rh(Cl)(CO)_3$. In view of the facility of the CO ejection/recombination processes it is suggested that such reaction pathways could be important in the substitution reactions of $\{Rh(Cl)(CO)_2\}_2$ and could aid the interpretation of the kinetic data. © 1998 Elsevier Science S.A.

*Keywords:* Bis-{chloro(dicarbonyl)rhodium}; Terminal carbonyl ligands; UV–visible

## 1. Introduction

Bis-{chloro(dicarbonyl)rhodium}, (I), [3] reacts thermally in solution by two principal processes: (a) ligand substitution and (b) bridge cleavage. With tertiary phosphines, an associative reaction is proposed to occur resulting in ligand exchange [8,9]. Eq. (1) illustrates the proposed reaction pathway.

* Corresponding author.
[1] On leave from Departamento de Quimica, Universidad Tecnica Federico Santa Maria, Casilla 110-V, Valparaiso, Chile.
[2] Also corresponding author.

[3] The solid state structure of $\{Rh(Cl)(CO)_2\}_2$ belongs to the $C_{2v}$ symmetry point group with an angle of 124°($\Theta$) between the two planes [1]. The distance between the Rh atoms (3.12 A) was initially thought to indicate Rh–Rh bonding [2,3] but further analysis of the structure and its energy levels suggested that the extent of the Rh–Rh bonding was limited [1,4,5]. Infrared spectra in the terminal CO stretching region are consistent with the $C_{2v}$ structure [6,7] but attempts to confirm this structure by conventional Raman spectroscopy failed because of the dark red colour of the complex [6].

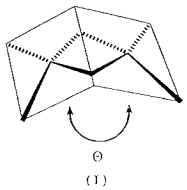


(I)

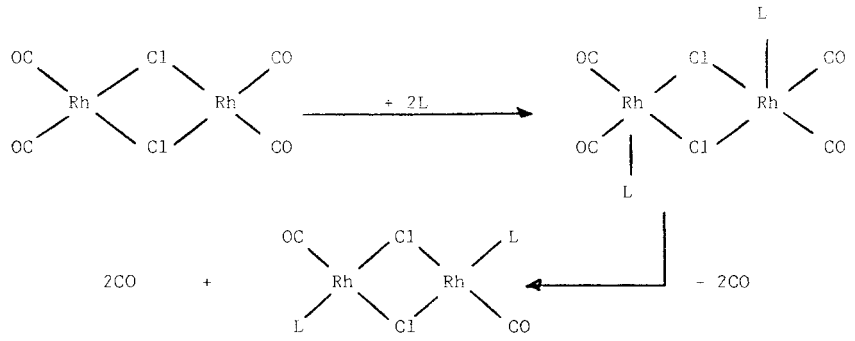


(1)

Bridge cleavage has been demonstrated in the reaction of $\{Rh(Cl)(CO)_2\}_2$ with tricyclohexylphosphine oxide, $Cy_3PO$ [8] and methylphenylphosphines $PPh_nMe_{3-n}$ ($n = 3$ and $n = 1$) [9]. The formation of the *cis*-dicarbonyl species by this process is illustrated in Eq. (2). In this case, it is proposed that there is addition of $Cy_3PO$, $PPh_3$ or $PPhMe_2$ followed by bridge cleavage because low temperature NMR spectroscopy demonstrated the existence of a very unstable pentacoordinated species $\{Rh(CO)_2(PPhMe_2)(\mu\text{-}Cl)\}_2$ as a reaction intermediate [9]. There appears, therefore, to be a common intermediate, involving addition of the incoming ligand, in Eqs. (1) and (2).

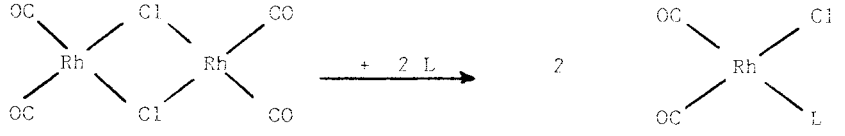


(2)

Despite the extensive applications of $\{Rh(Cl)(CO)_2\}_2$ as a catalyst in hydrogenation, hydroformulation, carbonylation and decarbonylation reactions [10], the only reported photochemistry of this compound is esr evidence for metal-centred radicals following 'homolytic cleavage of the Rh–Rh bond'. [4] Since $\{Rh(Cl)(CO)_2\}_2$ does not have a Rh–Rh bond the actual identity of the radicals referred to remains a mystery. The lack of photochemistry is somewhat surprising given that $\{Rh(Cl)(CO)_2\}_2$ contains carbonyl ligands which should be photochemically labile, as seen with other mononuclear Rh complexes, e.g., $Rh(L)_2(CO)(Cl)$ [12–14] and related metal carbonyl compounds [15,16]. It may well be, however, that the lack of such studies is related to the fact that studying 16 electron species is more difficult than 18 electron species and that excitation to a state which could give rise to substitution and/or bridge cleavage is rapidly followed by processes which return the system to the ground state.

In this paper, we report a study of $\{Rh(Cl)(CO)_2\}_2$ in frozen gas matrices (Ar, $CH_4$, $N_2$ and CO; 12 K) and Nujol solutions (77 K) in an attempt to determine the structures of species formed by irradiation. We relate the formation of these new species to transients proposed in solution reactions.

[4] See Ref. [11]; cited in Chem. Abs., 112 (1990) 87939g.

## 2. Experimental details

Details of the 12 K cryostat, its vacuum system, matrix gases, and the 125 W medium-pressure mercury arc photolysis lamp at Southampton have been described elsewhere [17]. Matrices containing $\{Rh(Cl)(CO)_2\}_2$ were prepared by subliming the complex (60 min, 298 K) and co-condensing the vapour with a large excess of matrix gas, i.e., the slow spray-on technique. Wavelength-selective photolyses were achieved using the following combinations of absorbing materials: filter A, $300 < \lambda < 370$ nm and $\lambda > 550$ nm, Pyrex glass disc (5 mm thick) + quartz gas cell (pathlength 25 mm) containing $Br_2$ (200 Torr); filter B, $\lambda < 370$ nm and $\lambda > 550$ nm, quartz gas cell (pathlength 25 mm) containing $Br_2$ (200 Torr); filter C, $\lambda > 400$ nm, Pyrex disc (5 mm thick) + quartz gas cell (pathlength 25 mm) containing $Cl_2$ (2 atm.). Infrared spectra were recorded using a computer-assisted grating spectrometer (Perkin Elmer 983G, resolution 1 $cm^{-1}$) with facilities for subtracting spectra [5] via a Perkin Elmer 3600 Data Station. Electronic absorption spectra were recorded using a Perkin Elmer Lambda 7 spectrometer which was also coupled into the 3600 Data Station.

The 77 K temperature studies at Idaho were carried out using a liquid nitrogen cooled glass cryostat designed at Southampton [18] and described in detail elsewhere [19]. Saturated Nujol solutions were prepared by grinding ca. 1 mg of $\{Rh(Cl)(CO)_2\}_2$ in a pestle and mortar and then adding approximately 25 drops of Nujol (Fischer Scientific) that had been degassed and then stored under nitrogen. The mixture was ground thoroughly to give the $\{Rh(Cl)(CO_2\}_2$ maximum opportunity to dissolve. After grinding the mixture was pipetted into a test tube and centrifuged for 20 min. Approximately 12 drops of the clear fluid was transferred by pipette from the test tube to the $CaF_2$ window assembly of the IR cell making sure not to transfer any solid sediment. With the sample in the IR cell, the Dewar assembly was purged for 10 min. After purging the assembly was alternately evacuated and purged five times to ensure a moisture-free environment before cooling. Such samples gave strong i.r. bands and could also be used for parallel UV–Visible studies. Wavelength-selective photolyses employed a 350 W high-pressure mercury-arc lamp (UVOP) and a quartz cell (pathlength 20 mm filled with $H_2O$) to remove unwanted heat and i.r. radiation together with the following combinations of absorbing materials: filter D, $250 < \lambda < 390$ nm, Hoya filter U330; filter E, $\lambda > 350$ nm, Corion filter LG-350; filter F, $350 < \lambda < 655$ nm, saturated solution of $CuSO_4$ (pathlength 10 mm) + saturated solution of $COCl_2$ (pathlength 10 mm). Infrared spectra were recorded using a Bio-Rad FTS-15/80 Fourier transform i.r. spectrometer connected to a Bio-Rad 3200 Work Station. Electronic spectra were obtained using a Cary 2200 UV–Visible spectrometer.

Raman spectra of $[\{Rh(Cl)(CO)_2\}_2]$ at Southampton were obtained on a Perkin Elmer Fourier transform Raman (FT Raman) spectrometer, powered by a Spectron laser system (Model 301; Nd/YAG source; $\lambda =$ 1064 nm), details of which have been comprehensively described elsewhere [20]. The spectra were corrected for filter and detector characteristics and hence the relative intensities of the bands are meaningful [21].

$\{Rh(Cl)(CO)_2\}_2$ was prepared according to the literature method [22] and had a satisfactory agreement with literature i.r. and UV–Visible spectroscopic characteristics [6,7,22,23].

## 3. Results

### 3.1. Electronic absorption spectra

UV–Visible spectra of $\{Rh(Cl)(CO)_2\}_2$ and its photoproducts were routinely recorded during experiments: (i) to monitor the course of reactions and to choose the appropriate wavelength-selective photolysis sources, e.g., an experiment with an Ar matrix (Fig. 1); and (ii) to look for relatively new strong bands which could be assigned to $\sigma \rightarrow \sigma^*$ transitions arising from M–M bonds in the photoproducts [15,16]. No such relatively strong bands were observed and thus it was concluded that the various photoproducts did not have Rh–Rh bonds. UV–Visible band positions are presented in Table 1.

### 3.2. Raman spectrum of $\{Rh(Cl)(CO)_2\}_2$

The FT Raman spectrum of $\{Rh(Cl)(CO)_2\}_2$ as a pure solid or diluted with KBr to minimise decomposition effects [24] showed clear sets of bands in the terminal CO stretching and ligand bending regions (Fig. 2a). An expansion of the terminal CO stretching region shows the four bands (Fig. 2b) expected for a $C_{2v}$ symmetry structure (I). These bands correlate well with bands and energy-factored CO stretching and interaction force constants determined by i.r. spectroscopy (Table 2) [6,7,25].

### 3.3. Photolysis of $\{Rh(Cl)(CO)_2\}_2$ in Ar, $CH_4$, $N_2$ and CO matrices at ca. 12 K

The i.r. spectrum of $\{Rh(Cl)(CO)_2\}_2$ isolated at high dilution in Ar, $CH_4$, $N_2$ and CO matrices at ca. 12 K showed the same of bands in the terminal CO stretching

[5] All subtractions were carried out in absorbance mode.

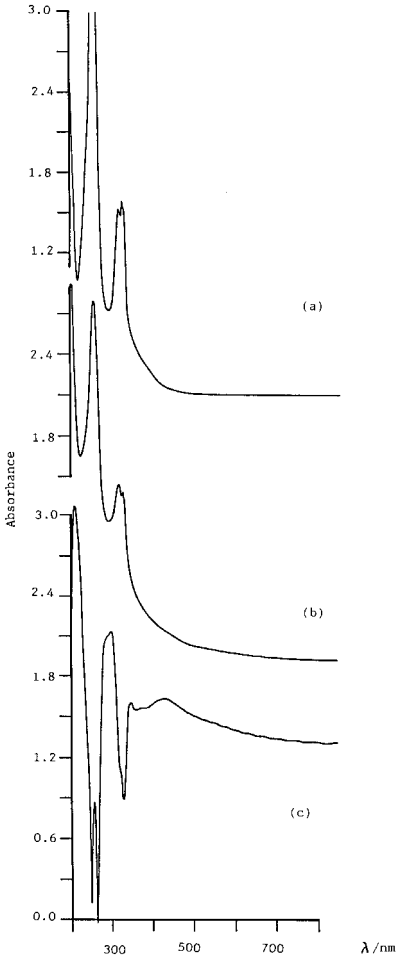


Fig. 1. Electronic spectra from an experiment with $\{Rh(Cl)(CO)_2\}_2$ isolated at high dilution in an Ar matrix at ca. 12 K: (a) after deposition; (b) after 15 h photolysis with UV radiation (filter B); (c) subtraction spectrum (b)-*A*(a), where *A* is a scaling factor.

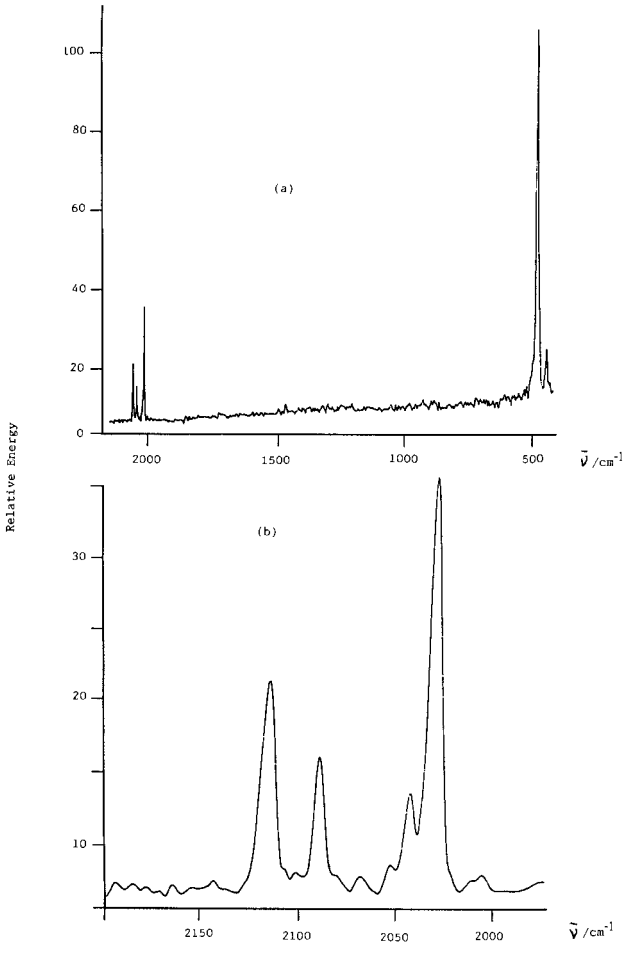


Fig. 2. FT Raman spectrum of $\{Rh(Cl)(CO)_2\}_2$ as a solid at 298 K: (a) full spectrum and (b) expansion of the CO stretching region.

region, e.g., the spectrum for an Ar matrix (Fig. 3a). The set of strong bands at 2111(m), 2093(s) and 2040(s) $cm^{-1}$ correlate with the bands observed in solution [6,7] and in Nujol mulls (Table 2). This establishes that the complex vapourises for matrix formation without decomposition and without any alteration to the bent molecular structure (I).

On photolysis in Ar with mid-UV light (filter A; 45 min), corresponding to the electronic absorption bands at 316 and 323 nm, a new electronic absorption peak was observed at 424 nm (Fig. 1b) together with new i.r. bands at 2139, 2101, 2035, 2029 and 2021 $cm^{-1}$ with

Table 1
Electronic absorption band positions ($\lambda_{max}$/nm) for $\{Rh(Cl)(CO)_2\}_2$ and its photoproducts in various media

| Species | Ar (12 K) | $CH_4$ (12 K) | $N_2$ (12 K) | CO (12 K) | Nujol (77 K) |
|---|---|---|---|---|---|
| $\{Rh(Cl)(CO)_2\}_2$ (I) | 258 | 254 | 258 | 260 | 265 |
| | 316 | 318 | 315 | 319 | 319 |
| | 323 | 328 | 323 | 323 | |
| $Rh_2(Cl)_2(CO)_3$ (XI) | 424 | –[a] | | | –[a] |
| $Rh_2(Cl)_2(CO)_3(N_2)$ (XII) | | | 404 | | |
| $\{Rh(Cl)(CO)_3\}_2$ (XX) | | | | 434 | |
| $Rh_2(Cl)_2(CO)_2$ (XVII) | –[a] | 431 | | | –[a] |

[a] Band too weak to observe or else obscured by bands of the parent compound.

Table 2
Infrared (IR) and Raman (R) active terminal CO stretching band positions ($\nu$/cm$^{-1}$) and energy-factored bond stretching ($K$) and interaction ($k_i$) force constants (Nm$^{-1}$)[a] for $\{Rh(Cl)(CO)_2\}_2$ in various media

| Band | Cyclohexane[b] solution, IR(298 K) | Solid[c] R (298 K) | Nujol IR (298 K) | Nujol IR (77 K) | $CH_4$ IR (12 K) |
|---|---|---|---|---|---|
| $A_1$ (IR, R) | 2105 | 2115 | 2105 | 2107 | 2109 |
| $B_1$ (IR, R) | 2089 | 2089 | 2089 | 2090 | 2092 |
| $B_2$ (IR, R) | 2034 | 2042 | 2033 | 2034 | 2036 |
| $A_2$ (R) | (2031)[d] | 2029 | e | e | e |

concomitant decreases in the intensities of the parent bands (Fig. 3b). The band at 2139 cm$^{-1}$ can be assigned to 'free' CO, i.e., a CO ligand has been ejected and the other bands correspond to terminal CO ligands. It is noteworthy that there are no bands in the region corresponding to bridging CO ligands. This is in contrast to the photoproducts observed for the dimeric complexes of the type $\{(\eta^5\text{-}C_5R_5)M(CO)_n\}_2$ (M = Fe, $n$ = 2; M = Mo, $n$ = 3; R = H, Me) which eject CO and form CO bridges simultaneously [26,27]. On further UV photolysis with light covering all three absorption bands (filter B) or just the highest energy band at 258 nm a similar steady growth in the set of new bands was observed.

On photolysis with visible radiation it was observed that slow back photolysis could be achieved with wavelengths as long as 690 nm but that photolysis proceeded more rapidly as higher energy radiation was used. Using

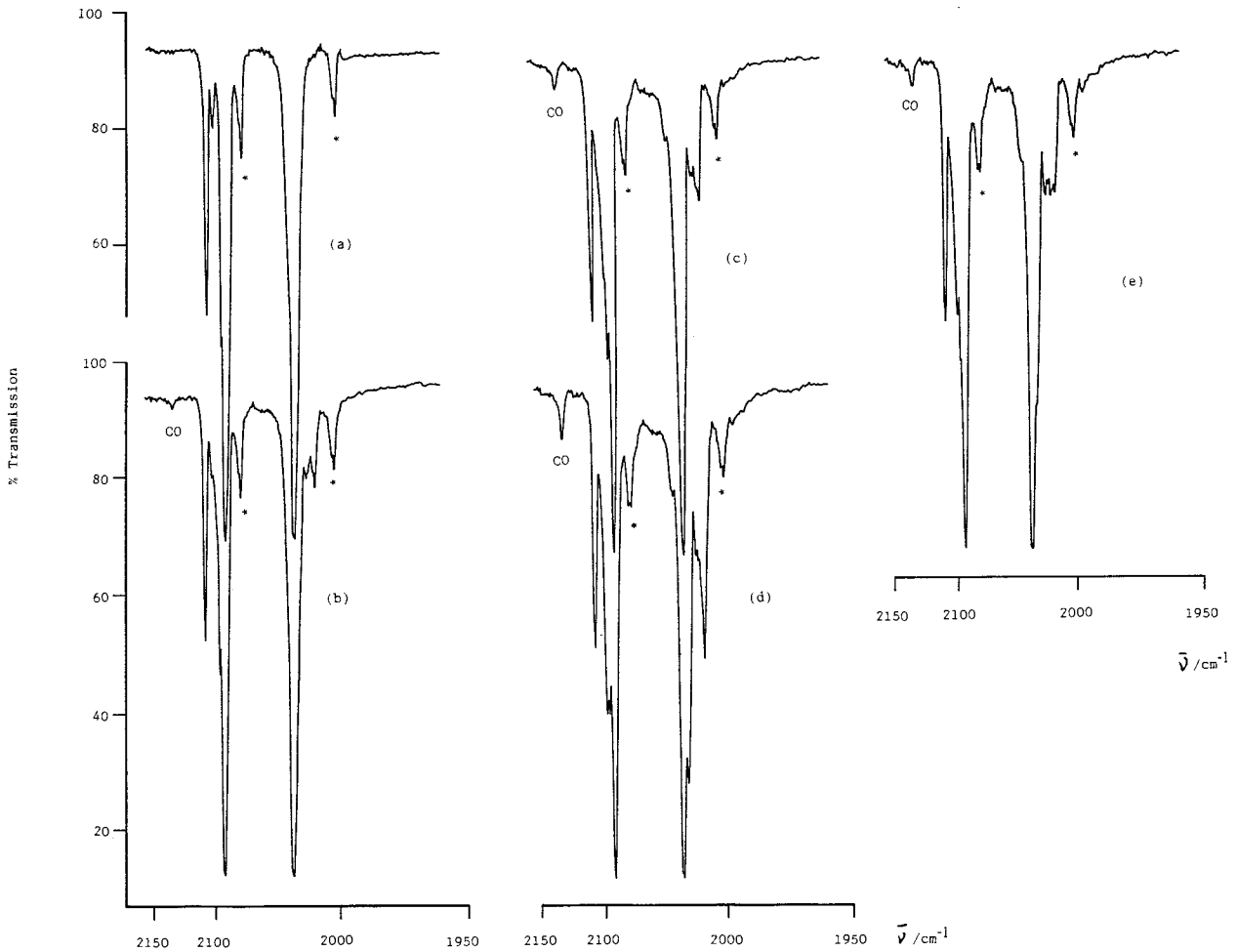


Fig. 3. I.r. spectra from an experiment with $\{Rh(Cl)(CO)_2\}_2$ isolated at high dilution in an Ar matrix at ca. 12 K: (a) after deposition, (b) after mid-UV irradiation (filter A; 45 min); (c) after further irradiation with the same radiation (15 h); (d) after UV irradiation(filter B, 30 min); (e) after irradiation with visible light (filter C, 45 min). Bands marked arise from $Rh_2(Cl)_2(^{12}CO)_3(^{13}CO)$ present in natural abundance.

an irradiation source covering the new electronic absorption band at 424 nm (filter C) photoreversal was quite rapid (Fig. 3c). Reversal could also be efficiently achieved by annealing the matrix to ca. 35 K. These reversals showed that the bands at 2101, 2035 and 2027 $cm^{-1}$ belonged to a different species, (II), to the species giving rise to the band at 2021 $cm^{-1}$, (III) (Tables 1 and 3).

Similar behaviour was observed with $CH_4$ matrices except that the forward photolysis proceeded more readily and extensively than in Ar matrices, which is a well-known phenomenon [28]. Surprisingly, no electronic absorption band was seen for (II) whereas there was a clear band for (III) at 431 nm (Tables 1 and 3).

Photolysis of $\{Rh(Cl)(CO)_2\}_2$ isolated at high dilution in $N_2$ matrices at ca. 12 K with mid-UV radiation (filter A, 5 min) produced a reduction in the parent bands and the growth of new i.r. bands at 2256, 2139, 2105, 2045, 2041 and 2024 $cm^{-1}$ (Fig. 4a,b). Further irradiation (filter A) resulted in the gradual increase in these bands together with new bands at 2242, 2214, 2050 and 2032 $cm^{-1}$ (Fig. 4c). Irradiation with higher energy radiation (filter B) produced a faster conversion of $\{Rh(Cl)(CO)_2\}_2$ to its photoproducts. Attempts at reversal with visible light ($\lambda > 430$ nm) were unsuccessful but efficient reversal was achieved with light corresponding to the new electronic absorption band (404 nm; filter C) and by annealing the matrix. The new band at 2139 $cm^{-1}$ ('free' CO) clearly indicates the ejection of CO while the bands at 2256, 2242 and 2214 $cm^{-1}$ correspond to terminal NN stretching modes [29]. The remaining bands can be assigned to terminal CO stretching bands of the mono-substituted, (IV), and possibly the di-substituted(V–VII) dinitrogen complexes (see Section 4).

On photolysis (filter A) of $\{Rh(CL)(CO)_2\}_2$ in CO matrices new weak i.r. bands were observed at 2104, 2064 and 2031 $cm^{-1}$. Similar bands were obtained on UV photolysis (filter B). No reversal was achieved on irradiation with visible light despite the appearance of a new electronic absorption band at 434 nm (Table 1) and no reversal was observed on annealing the matrices to ca. 40 K. At higher annealing temperatures the CO was pumped off the cold window due to its finite vapour pressure above 40 K. The assignment of the new i.r. bands to monomeric, (VIII), or dimeric, (IX), products is discussed below (see Section 4).

### 3.4. Photolysis of $\{Rh(Cl)(CO)_2\}_2$ in Nujol mulls at ca. 77 K

At 298 K, the i.r. spectrum of $\{Rh(Cl)(CO)_2\}_2$ in a Nujol mull exhibits three bands in the terminal CO stretching region at 2105, 2089, and 2033 $cm^{-1}$ which are in agreement with the band positions for cyclohexane solutions [7] and $CH_4$ matrices, which are also hydrocarbon media (Table 2). Upon cooling the mull to ca. 77 K the bands shifted by 1 $cm^{-1}$ to higher wavenumbers (Table 3).

Photolysis of the mulls with mid-UV radiation (filter D; 30 min) produced new i.r. bands at 2131 ('free' CO), 2094, 2026, and 2018 $cm^{-1}$ (Fig. 5b). These bands correspond to those observed for Ar and $CH_4$ matrices (Table 3). Back photolysis (filter C; 45 min; Fig. 5c) or annealing the mull by allowing a warm-up to ca. 180 K and then re-cooling to 77 K in order to record the i.r.

Table 3
Terminal CO stretching band positions ($\nu$/$cm^{-1}$) for $\{Rh(Cl)(CO)_2\}_2$ and its photoproducts in various low temperature media

| Species | Structure | Ar (12 K) | CH4 (12 K) | N2 (12 K) | CO (12 K) | Nujol (77 K) |
|---|---|---|---|---|---|---|
| $\{Rh(Cl)(CO)_2\}_2$ (I) | (I) | 2111 | 2109 | 2113 | 2113 | 2106 |
| | | 2093 | 2092 | 2097 | 2097 | 2090 |
| | | 2040 | 2036 | 2043 | 2042 | 2034 |
| $Rh_2(Cl)_2(CO)_3$ (II) | (XI) | 2101 | 2098 | | | 2094 |
| | | 2035 | 2030 | | | 2026 |
| | | 2029 | 2023 | | | 2018 |
| $\{Rh(Cl)(CO)\}_2$ (III) | (XVII) | 2024 | 2021 | | | |
| | | 2021 | 2011 | | | |
| $Rh_2(Cl)_2(CO)_3(N_2)$[a] (IV) | (XII) | | | 2113 | | |
| | | | | 2097 | | |
| | | | | 2042 | | |
| $Rh_2(Cl)_2(CO)_2(N_2)_2$[b] | (XV) | | | —[c] | | |
| $Rh_2(Cl)_2(CO)_2(N_2)_2$[d] | (XVI) | | | 2052 | | |
| | | | | 2032 | | |
| $\{Rh(Cl)(CO)_3\}_2$ | (XX) | | | | 2104 | |
| | | | | | 2064 | |
| | | | | | 2031 | |

[a] NN stretching band at 2256 $cm^{-1}$.
[b] NN stretching bands at 2242 and 2214 $cm^{-1}$.
[c] CO stretching bands obscured by bands of (I).
[d] NN band overlapped by band of (XII) at 2256 $cm^{-1}$.

spectrum, resulted in increases in intensity of all the bands of the parent complex and decreases in the intensities of the product bands (Fig. 5d).

## 4. Discussion

### 4.1. Structure of $\{Rh(Cl)(CO)_2\}_2$

The combined i.r. and Raman spectroscopic evidence establishes that at 298 K $\{Rh(Cl)(CO)_2\}_2$ has a bent structure, (I), with $C_{2v}$ symmetry.

### 4.2. Matrix photoproducts

The photoreactions are summarised in Scheme 1.

#### 4.2.1. Structures of the CO-loss products

In Ar, $CH_4$ and $N_2$ matrices and Nujol mulls it is apparent that photo-ejection of CO occurs without any terminal to bridging rearrangement of the remaining CO ligands and with retention of the $\{Rh_2Cl_2\}$ bridging unit, cf. the low temperature NMR study [9]. Based on structure (I), the fragments that are produced must have: (a) a vacant site, e.g., (X); (b) a matrix molecule (M) occupying the vacant site and interacting weakly with an Rh atom as a solvent molecule might do in solution at 298 K, e.g., (XI); (c) a matrix molecule acting as a ligand (L), occupying the vacant site and forming a definite bond with the Rh atom as in a substitution complex, e.g., (XII) with $L = N_2$; (d) undergone an oxidative addition reaction with a C–H bond of $CH_4$ and Nujol, e.g., (XIII); (e) adopted a 3-coordinate geometry for the Rh atom losing CO, i.e., (XIV), rather than having a 4-coordinate geometry at the vacant site as in (X).

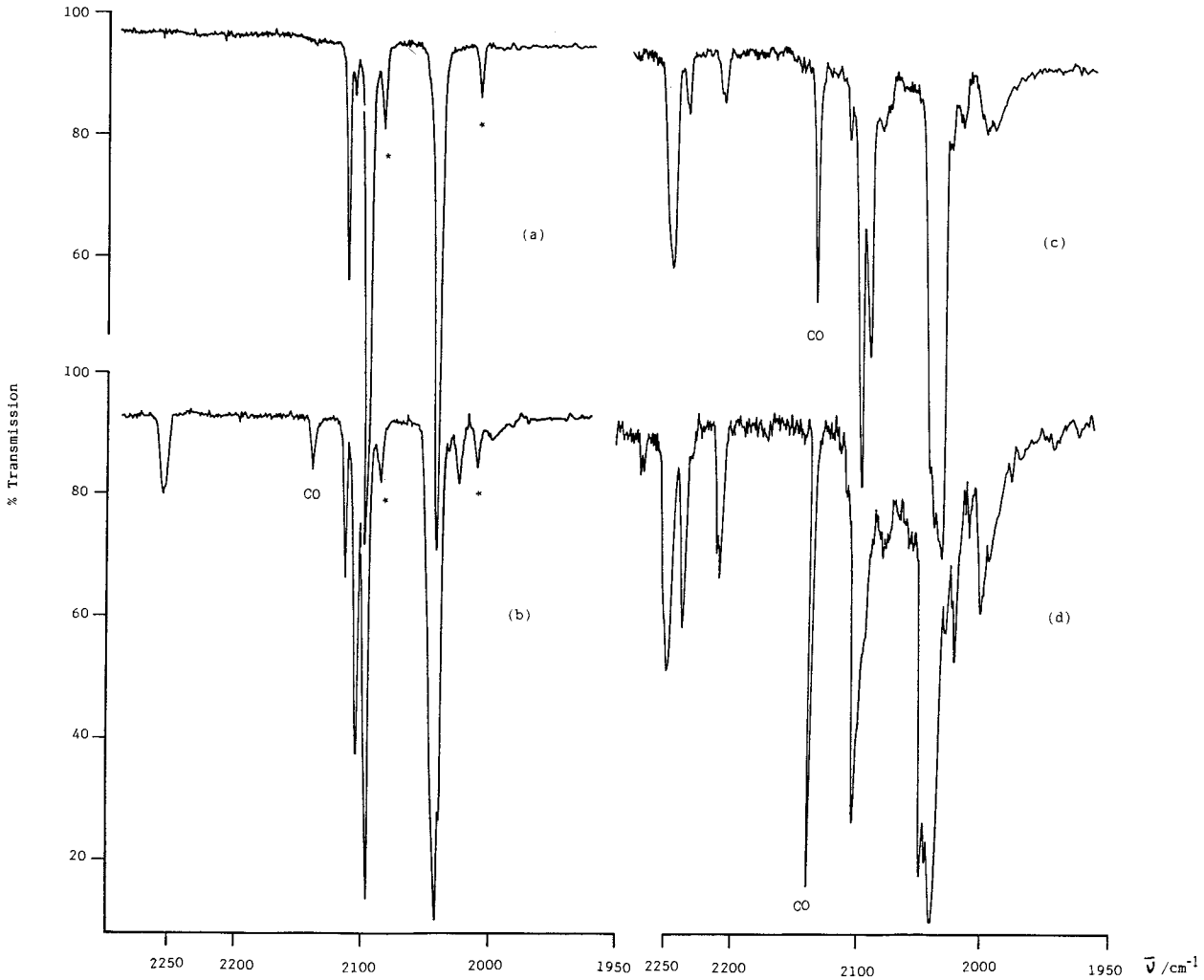


Fig. 4. I.r. spectra from an experiment with $\{Rh(Cl)(CO)_2\}_2$ isolated at high dilution in a $N_2$ matrix at ca. 12 K: (a) after deposition, (b) after mid-UV irradiation (filter A, 5 min), (c) after further mid-UV irradiation (filter A, 55 min), and (d) after UV irradiation (filter B, 120 min). Bands marked * correspond to $Rh_2(Cl)_2(^{12}CO)_3(^{13}CO)$ present in natural abundance.

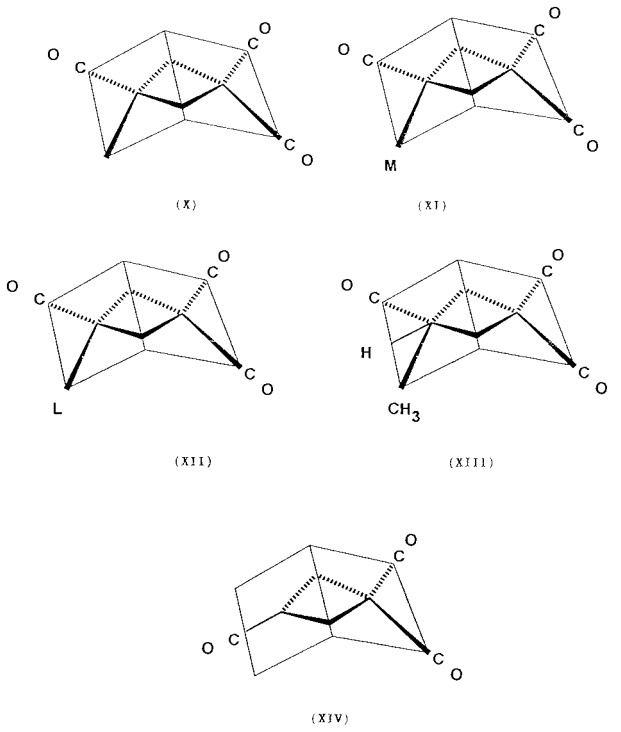


In the event of secondary photolysis, dicarbonyl species could be formed with *gem*(XV), *cis*(XVI), *trans*(XVII) and (XVIII) CO bonds.

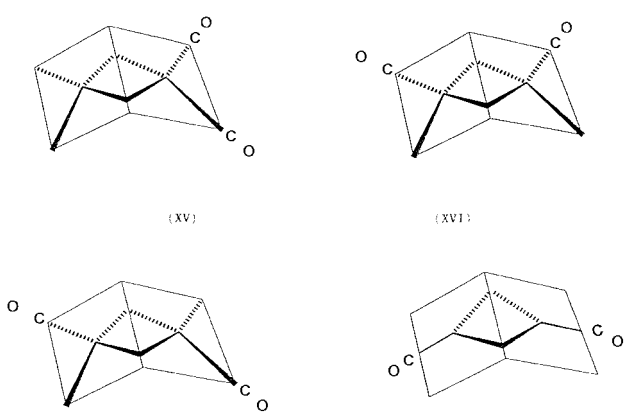


The fact that the energy-factored CO-stretching force constants, $k_{cis}$ and $k_{trans}$, for (I) are so small (Table 2) means that, to a first approximation, local symmetry and bonding arguments can be applied to each Rh atom. Thus, in (X), (XI), (XII), (XIII) and (XIV) the $Rh(CO)_2$ fragments will give rise to symmetric and antisymmetric CO stretching bands, which will be relatively independent of the changes on the other Rh atom. The Rh(CO) fragments, however, will have single CO stretching modes which are highly dependent on whether there is a vacancy, a weakly interacting matrix molecule, a $N_2$ ligand, or there has been oxidative addition or structural rearrangement.

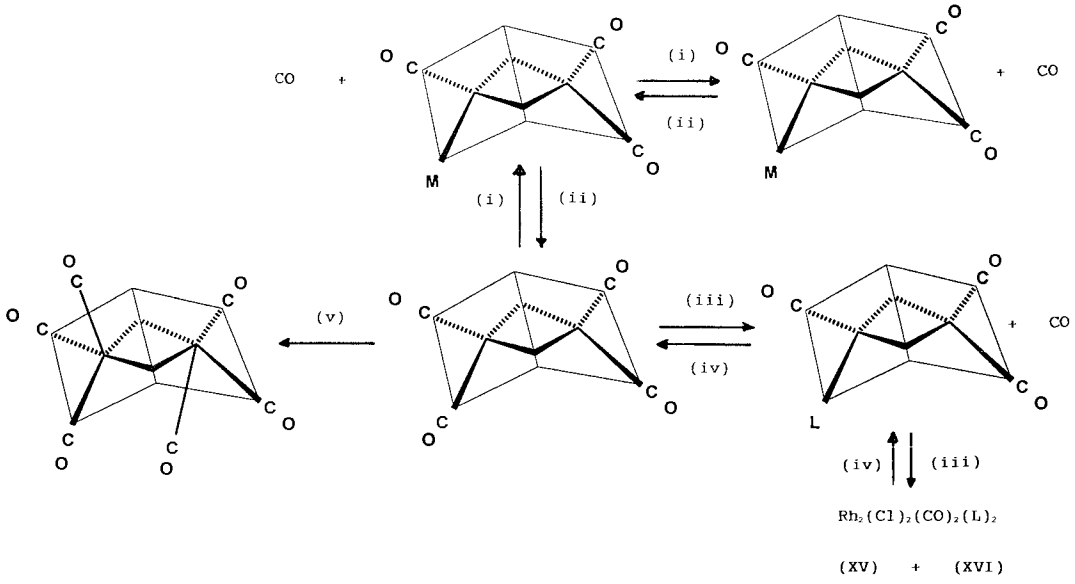


Scheme 1. (i) $h\nu$ (filter A{300 < λ < 370 nm and λ > 550 nm} for Ar and $CH_4$; filter D{250 < λ < 390 nm} for Nujol); (ii) $h\nu$ (filter C{λ > 400 nm} for Ar and $CH_4$; filter E{λ > 350 nm} for Nujol); (iii) $h\nu$ (filter A for $N_2$); (iv) $h\nu$ (filter C or annealing for $N_2$);2 (v) $h\nu$ (filters A and C for CO).

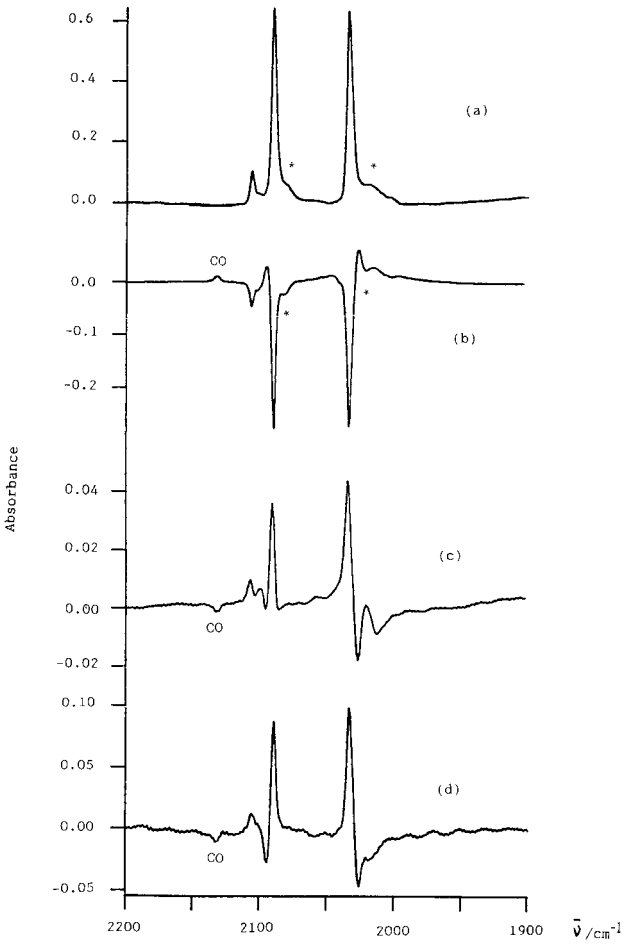


Fig. 5. I.r. spectra from an experiment with $\{Rh(Cl)(CO)_2\}_2$ dispersed in a Nujol mull: (a) at 77 K, (b) after 30 min mid-UV irradiation (filter D) minus starting material (subtraction spectrum (b), $A$(a) where $A$ is a scaling factor); (c) after 45 min back photolysis (filter C); (d) after annealing the mull to −100°C minus back photolysis (subtraction spectrum (d), $C$(c) where $C$ is a scaling factor). Bands marked * correspond to $Rh_2(Cl)_2(^{12}CO)_3(^{13}CO)$ present in natural abundance.

The close correspondence of the set of three bands for Ar (2101, 2035 and 2029 cm$^{-1}$), $CH_4$ (2098, 2030 and 2023 cm$^{-1}$) and Nujol (2094, 2026 and 2018 cm$^{-1}$) indicates a common structure, i.e., (X) or (XI), rather than a species formed by C–H activation in the case of $CH_4$ or Nujol, i.e., structure (XIII) can be discounted. This is supported by the widely different terminal CO stretching band positions for ($\eta^5$-$C_5H_5$)Ir(CO) (1953.7 cm$^{-1}$, Ar) and ($\eta^5$-$C_5H_5$)Ir(CO)(Me)(H) (2006.0 cm$^{-1}$, $CH_4$) [30]. The actual differentiation between structures (X) or (XI) is more difficult to make. On the one hand the species $Fe(CO)_4$ and $Fe(CO)_4 \ldots CH_4$ had very different i.r. band positions [31] whereas the $M(CO)_5 \ldots$ matrix molecules (M = Cr, Mo and W; matrix molecule = Ar, Kr, Xe, $CH_4$, $CF_4$ and $SF_6$) had similar i.r. band positions but dramatically different electronic absorption bands [32]. On the basis of the new visible band in an Ar matrix (424 nm) it seems possible [6] that the primary CO-loss species for Ar and $CH_4$ adopts the weak interaction structure ((XI) = (II)) while the species in $N_2$ adopts structure (XII).

Considering the various dicarbonyl species, it would be expected that *gem* species based on structure (XV) would have two terminal CO stretching bands separated by ca. 65 cm$^{-1}$ on the basis of $K = 1725$ and $k_{gem} = 55$ nm$^{-1}$(Table 2). *Cis* and *trans* species (XVI), (XVII) and (XVIII), on the other hand, would be expected to have two bands separated by ca. 12 cm$^{-1}$ (using $K =$ 1725 and $k_i = 10$ Nm$^{-1}$ from Table 2). Further differentiation can be made on the basis of relative band intensities: (XVI) would be expected to have $I_{symm}:I_{antisymm}$ = ca. 1, whereas the structures (XVII) and (XVIII) would be expected to have $I_{symm} < I_{antisymm}$. Examination of the data for (III) suggests structure (XVII) because the band separation is ca. 10 cm$^{-1}$ and the ratio $I_{symm}:I_{antisymm}$ is less than 1.

In the case of the bis-dinitrogen substituted species it has to be noted that NN interaction stretching force constants for monomeric species are less than CO interaction force constants, e.g., for $Ni(CO)_2(N_2)_2$: $k_{CO,CO}$ = 79.6 Nm$^{-1}$; $k_{NN,NN}$ = 22.9 Nm$^{-1}$ [33]. In dimers, therefore, if $k_{br,CO,CO}$ is ca. 10 Nm$^{-1}$ (Table 2) then $k_{NN,NN}$ is likely to be less than 5 Nm$^{-1}$, i.e., possibly too small to give a splitting which could be differentiated from a 'matrix splitting effect' [29]. On the basis of the pair of NN stretching bands at 2242 and 2214 cm$^{-1}$ belonging to a mononuclear $M(N_2)_2$ fragment, it seems reasonable that in a $Rh_2(Cl)_2(CO)_2(N_2)_2$) species with structure (XV), the CO stretching bands for the $Rh(Cl)(CO)_2$ fragment could be very close to the bands for $\{Rh(Cl)(CO)_2\}_2$ and could thus not be observed. The pair of CO stretching bands at 2050 and 2032 cm$^{-1}$ is more in keeping with structures (XVI) and (XVII) and in these cases the expected NN stretching bands of $Rh(Cl)(CO)(N_2)$ fragments could be masked by the strong NN stretching band of the mono-substituted species $Rh_2(Cl)_2(CO)_3(N_2)$. In this case the interaction force constant ($k_i$ = 14.87 Nm$^{-1}$) is similar to the value of $k_c$ for $\{Rh(Cl)(CO)_2\}_2$ and this suggests the *cis* structure, (XVI) in contrast to the dicarbonyl CO loss products in Ar, $CH_4$ and Nujol which are suggested to have the *trans* structure (XVII). [7]

[6] An attempt to provide further information about possible agostic interactions using a $CF_4$ matrix was unsuccessful because insufficient photoproduct was obtained to get a UV–Visible spectrum.

[7] In making these assignments, several weak bands have not been explained, e.g., the 2024 cm$^{-1}$ terminal CO band in $N_2$. For the $N_2$ experiments a second CO stretching band corresponding to the CO stretching band at 2024 cm$^{-1}$ for a *trans* structure (XVII) could be obscured as could the weak NN stretching bands.

*4.2.2. Structure of the CO-gain product*

The photolysis of mononuclear organometallic species in CO matrices has been found to give species in which CO has replaced a ligand or CO has added at the expense of a bound ligand, e.g., a polyene ligand has changed its binding from $\eta^4$ to $\eta^2$ [34] while irradiation of dimers in CO matrices has led to bridge cleavage [26,27]. In the case of $\{Rh(Cl)(CO)_2\}_2$ two types of products could be anticipated: (i) CO addition products where CO adds to the coordinatively and electronically deficient Rh atoms to give (XIX) and (XX); and (ii) a mononuclear square planar product $Rh(Cl)(CO)_3$, (XXI). These species are analogous to the known dimer $Rh_2(Cl)_2(CO)_2(OPCy_3)_2$, which is proposed to adopt the *trans* structure, cf. (XX), and the monomeric species *cis*-$Rh(Cl)(CO)_2(OPCy_3)$ [1], *cis*-$Rh(Cl)(CO)_2(PR_3)$ (R = Me, Ph) [35,36], and *cis*-$Rh(Cl)(CO)_2$(amine) [37], cf. (XXI).

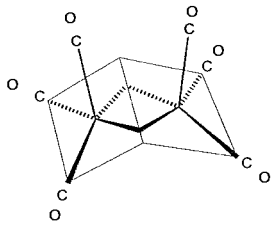

(XIX)

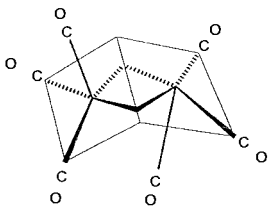

(XX)

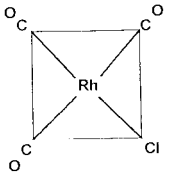


For the structure of the OPCy3 dimer, two i.r. active terminal CO stretching bands were observed at 2090 and 2008 $cm^{-1}$ whereas *four* bands would have been expected on the basis of $C_s$ symmetry. Adding CO ligands to (I) in a *transoid* fashion to give (XX) effectively produces two separate $Rh(CO)_3$ fragments with $C_s$ symmetry which would be expected to generate *three* i.r. bands of comparable relative intensities. The monomeric species (XXI) (L = CO) has $C_{2v}$ symmetry and this too would be expected to show three i.r. terminal CO stretching modes but in this case the upper $A_1$ mode, which corresponds to the symmetric stretching of the two *trans* CO ligands will have very low intensity because the change in dipole moment will be very small in a planar molecule. Only two i.r. terminal CO stretching bands would, therefore, be expected for (XXI). On the basis of a *three* rather than a *two* band pattern and energy-factored force-field fitting procedures [25], including comparisons of the energy-factored CO stretching and interaction force constants for $Rh_2(Cl)_2(CO)_2(OPCy_3)_2$ [1] and *cis*-$Rh(Cl)(CO)_2(L)$ (L = $OPCy_3$ [8,9], $PMe_3$ [35,36], and $PPh_3$ [35,36]), the bands at 2101, 2064 and 2031 $cm^{-1}$ seem better assigned as arising from a dimeric species $\{Rh(Cl)(CO)_3\}_2$ with structure (XX).

It is unfortunate that the CO matrices boil off before any secondary thermal reactions could be observed. A possible way round this in a future study would be to dope a Nujol mull with excess phosphine because Nujol mull media can be annealed almost to ambient temperature.

*4.3. Relevance of the low temperature photoreactions*

The resilience of the chlorobridges in this work supports the reaction path in Eq. (1) rather than a path which involves initial cleavage of the bridges to give 14-electron fragments, $Rh(Cl)(CO)_2$. A surprising feature of the present work was, however, the facile ejection and recombination of CO ligands and the addition of $N_2$. This indicates that the CO-loss pathway, though perhaps not the most obvious pathway, could also be playing a significant part in the ligand substitution reactions of $\{Rh(Cl)(CO)_2\}_2$ perhaps with solvent participation via coordination at the vacant site. Alternatively, it may well be argued that the photochemical processes observed in low temperature media are not important for reactions at ambient temperatures because deactivation processes deplete the concentration of the excited state species before chemical reactions can occur. For example, the presence of the heavy atoms Cl and Rh in the complexes can result in energy transfer to a chemically non-reactive state or to the ground state [38]. Further work using flash photolysis and IR detection would be useful in elucidating the importance of the CO loss pathway.

## 5. Conclusions

Low temperature spectroscopic studies (i.r. and UV–Visible) of $\{Rh(Cl)(CO)_2\}_2$ in gas matrices at ca. 12 K and Nujol mulls at ca. 77 K have shown that reversible CO ejection is such a facile process that such a reaction pathway may be playing an important part in the substitution reactions of this complex and perhaps other halo-bridged complexes.

## Acknowledgements

The Idaho group thanks the National Science Foundation under Grant No. RII-8902065 (University of Idaho) and the University of Idaho for a travel grant (to

A.J.R) under the EPSCoR programme. The Southampton group thank the Universidad Tecnica Federico Santa Maria for study leave (to M.A.O.), the British Council for support (to M.A.O.) under the Academic Link Scheme, the S.E.R.C. for support (to A.J.R.) and Dr. P.J. Hendra for making available time on FT Raman equipment at Southampton. We also thank NATO for a Travel Grant (to T.E.B. and A.J.R.) to enable the interchange of staff and research students.

## References

[1] R.H. Summerville, R. Hoffman, J. Am. Chem. Soc. 98 (1976) 7240.
[2] J.L. Balch, B. Tulyathan, Inorg. Chem. 16 (1972) 57.
[3] L.F. Dahl, C. Martell, D.L. Wampler, J. Am. Chem. Soc. 83 (1961) 1761.
[4] P.S. Braterman, Struct. Bond. (Berlin) 16 (1972) 57.
[5] P.S. Braterman, J. Am. Chem. Soc. 99 (1977) 1446.
[6] F.A. Cotton, C.S. Kraihanzel, J. Am. Chem. Soc. 84 (1962) 4432.
[7] B.F.G. Johnson, J. Lewis, P.W. Robinson, J. Chem. Soc. (A) (1968) 2693.
[8] P. Uguagliati, G. Deganello, U. Belluco, Inorg. Chim. Acta 9 (1974) 203.
[9] E. Rotondo, G. Battaglia, G. Giordano, F.P. Cusmano, J. Organomet. Chem. 450 (1993) 245.
[10] J. Halpern, Adv. Chem. Ser. 70 (1969) 1.
[11] J.H. Yuan, G. Xu, R. Chen, Bopuxue Zazhi 6 (1989) 187.
[12] W.T. Boese, A.S. Goldman, Organometallics 10 (1991) 782.
[13] C.T. Spillett, P.C. Ford, J. Am. Chem. Soc. 111 (1989) 1932.
[14] J.A. Maguire, A. Petrillo, A.S. Goldman, J. Am. Chem. Soc. 114 (1992) 9492.
[15] M.S. Wrighton, Chem. Rev. 74 (1974) 401.
[16] G.L. Geoffroy, M.S. Wrighton, Organomet. Photochem., Academic Press, London, 1975.
[17] A.J. Rest, I. Whitwell, W.A.G. Graham, J.K. Hoyano, A.D. McMaster, J. Chem. Soc., Dalton Trans. (1987) 1181.
[18] R.H. Hooker, PhD Thesis, Univ. of Southampton, 1989.
[19] K.A. Lott, T.E. Bitterwolf, J. Mascetti, A.J. Rest, J. Organomet. Chem. 419 (1991) 113.
[20] G. Ellis, P.J. Hendra, C.M. Hodges, T. Jawhari, C.H. Jones, P. Le Barazer, C. Passingham, I.A.M. Royard, A. Sanchez-Blasquey, G.M. Warnes, Analyst 114 (1989) 1061.
[21] D.J. Cutler, Spectrochim. Acta 46A (1990) 131.
[22] J.A. McCleverty, G. Wilkinson, Inorg. Synth. 8 (1965) 211.
[23] J.G. Bullitt, F.A. Cotton, Inorg. Chim. Acta 5 (1971) 637.
[24] T.N. Day, P.J. Hendra, A.J. Rest, A.J. Rowlands, Spectrochim. Acta 47A (1991) 1251.
[25] P.S. Braterman, Metal Carbonyl Spectra, Academic Press, London, 1975.
[26] P.E. Bloyce, A.K. Campen, R.H. Hooker, A.J. Rest, N.R. Thomas, T.E. Bitterwolf, J.E. Shade, J. Chem. Soc. Dalton Trans. (1990) 2833.
[27] M.L. Baker, P.E. Bloyce, A.K. Campen, A.J. Rest, T.E. Bitterwolf, J. Chem. Soc., Dalton Trans. (1990) 2825.
[28] M. Poliakoff, J. Chem. Soc., Faraday Trans. II 73 (1977) 569.
[29] R.B. Hitam, K.A. Mahmoud, A.J. Rest, Coord. Chem. Rev. 55 (1984) 1.
[30] A.J. Rest, I. Whitwell, W.A.G. Graham, J.K. Hoyano, A.D. McMaster, J. Chem. Soc., Dalton Trans. (1987) 1181.
[31] M. Poliakoff, J.J. Turner, J. Chem. Soc., Dalton Trans. (1974) 2276.
[32] R.N. Perutz, J.J. Turner, J. Am. Chem. Soc. 97 (1975) 4791.
[33] H. Huber, E.P. Kundig, M. Moskovits, G.A. Ozin, J. Am. Chem. Soc. 95 (1973) 332.
[34] S.T. Astley, M.P.V. Churton, R.B. Hitam, A.J. Rest, J. Chem. Soc. (1990) 3243.
[35] J. Gallay, D. De Montauzon, R. Poilblanc, J. Organomet. Chem. 38 (1972) 179.
[36] H.B. Tinker, D.E. Morris, J. Organomet. Chem. 52 (1973) C55.
[37] J.W. Kang, P.M. Maitlis, Can. J. Chem. 46 (1968) 897.
[38] R.P. Wayne, Principles and Applications of Photochemistry, Oxford Science Series, Oxford Univ. Press, Oxford, 1988.